# Estimating Fracture Toughness from Nonlinear Load-Deflection Relation*

K. KOMATSU**, H. SASAKI** and T. MAKU**

**Abstract**——Load- deflection relation of Double Cantilever Beam (DCB) specimens with thick epoxy adhesive layer was analyzed by assuming adherends to be elastic beam supported on a viscoelastic foundation. Method of analysis for the beam on elastic foundation was extended to the time dependent problem and numerical method based on the finite difference method was used. As the results of numerical calculations, it was clarified that while DCB specimen bonded with epoxy adhesives containing 0 and 20 phr of flexibilizer did not show the nonlinearity on load-deflection curve, those with 40 and 60 phr of flexibilizer showed the slight nonlinearity. Strain energy release rate of the DCB specimen was calculated from the load-deflection relation by employing the least squares method. Fracture toughness was estimated with experimental data and the derived equations of strain energy release rate. Other time independent methods for estimating fracture toughness of DCB specimen were also used, and results obtained by these all estimation methods were compared with each other. In consequence, no clear distinction between two kinds of fracture toughness estimated with time dependent equation and time independent equation was observed, because the relaxation time of epoxy adhesive was relatively large.

## Introduction

In the authors' previous paper[1], a method for estimating fracture toughness $G_c$ of double cantilever beam (DCB) specimen as shown in Fig. 1 was presented. The method was derived by assuming that the adhesive layer behaved like infinite rows of elastic springs, and fracture toughness $G_c$ was estimated with equation involving elastic constants of materials and fracture load by assuming that the linearity of load-deflection ($P-\delta$) relation was kept till fracture. In reality, however, nonlinearity of $P-\delta$ relation was observed in that test, so it was supposed that the estimation method involved some amount of error coming from the above mentioned assumption.

In this study, it was intended to make sure of the difference between fracture toughness $G_c$ estimated under the assumption of linear $P-\delta$ relation and that estimated under the assumption of nonlinear $P-\delta$ relation. For this purpose, effort was made on expressing the nonlinear $P-\delta$ relation by assuming a linear

* This paper is defined as "Studies on the Opening Mode Fracture Toughness of Wood-Epoxy Adhesive System (II)." The previously reported paper "Strain Energy Release Rate of Double Cantilever Beam Specimen with Finite Thickness of Adhesive Layer" is denoted herewith also as "Studies on the Opening Mode Fracture Toughness of Wood-Epoxy Adhesive System (I)."

** Division of Composite Wood.

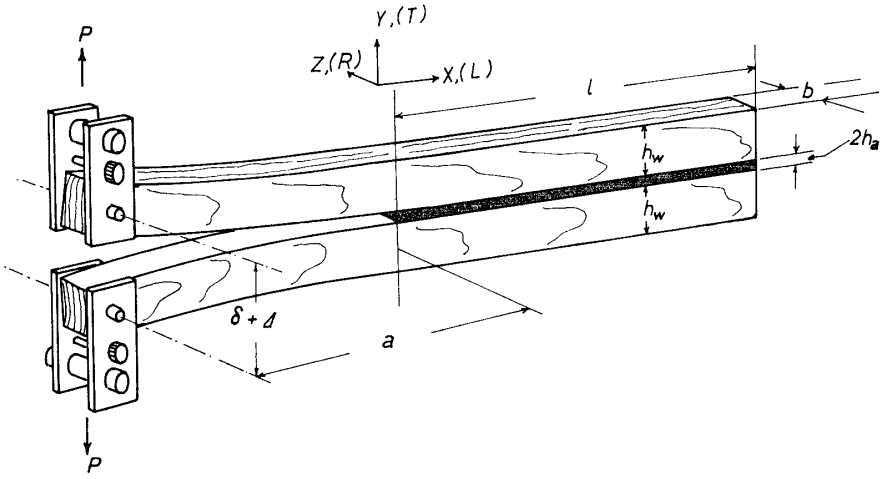


Fig. 1. Double Cantilever Beam (DCB) specimen with thick adhesive alyer. a: crack (beam) length, $l$: glue line length, $h_w$: depth of beam, b: thickness of specimen, $2h_a$: thickness of glue line, $\Delta = 2h_a + h_w$, P: load, $\delta$: deflection.

viscoelastic material for the adhesive layer, and three elements model was used for the simplicity of the analysis. The principle of solution in this case was the same as the previous paper[1] concerning to elastic adhesive layer, but the process of the analysis was somewhat complicated, so that calculations based on the finite difference method and least squares method were adopted.

## Theory

*Derivation of Basic Differential Equation of DCB Specimen*

Fig. 2 shows schematic relations of lower half DCB specimen with an adhesive layer of finite thickness. In this figure, it was assumed that the wood adherend in the upper side of the neutral axis of bending in region-2 deformed in y-direction and the mechanical behaviour of this part was simulated by infinite rows of elastic springs of which modulus of elasticity was $E_y$. As good results were obtained in

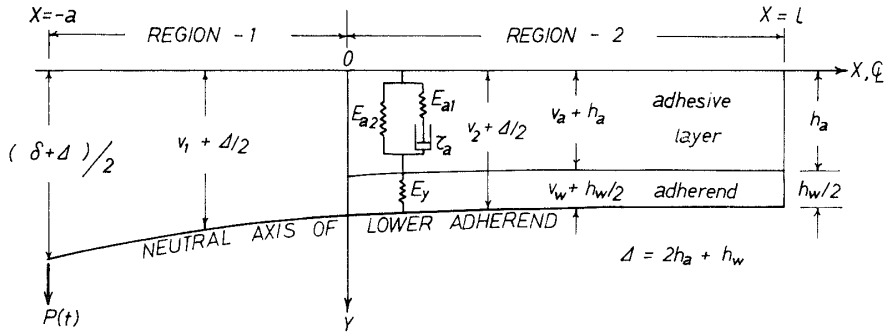


Fig. 2. Schematic relation of DCB specimen. $v_a$: elongation of adhesive layer, $v_w$: elongation of wood adherend, $v_2$: deflection of the neutral axis ($=v_a+v_w$) in region-2, $v_1$: deflection in region-2.

the previous paper[1] by this assumption, the same assumption was taken again here. Thus stress-strain relation of wood adherend in y-direction is

$$\varepsilon_w = \sigma_y / E_y, \tag{1}$$

$$\varepsilon_w = v_w / 0.5h_w, \tag{2}$$

and

$$\sigma_y = q/b, \tag{3}$$

where, $\varepsilon_w$ is y-directional strain of wood adherend, $v_w$ is y-directional elongation of wood adherend, and $h_w$ is depth of single cantilever beam, $\sigma_y$ is y-directional stress acting in common with wood adherend and adhesive layer, q is distributing force per unit length in x-direction, and b is thickness of secimen.

It was also assumed that the mechanical behaviour of adhesive layer could be simulated by infinite rows of three elements mechanical model as shown in Fig. 2 The relation between nomal stress $\sigma_y$ and normal strain $\varepsilon_a$ can be expressed by the following differential equation.

$$\frac{\partial \sigma_y}{\partial t}(x, t) + \frac{\sigma_y}{\tau_a}(x, t) = (E_{a1} + E_{a2}) \frac{\partial \varepsilon_a}{\partial t}(x, t) + \frac{E_{a2}}{\tau_a} \varepsilon_a(x, t), \tag{4}$$

where, $\tau_a$ is relaxation time of Maxell element, $E_{a1}$ and $E_{a2}$ are modulus of elasticity of spring element, and t is time. Approximating the strain of adhesive layer $\varepsilon_a$ by the conventional strain:

$$\varepsilon_a = v_a / h_a, \tag{5}$$

where, $v_a$ and $h_a$ are elongation and half thickness of adhesive layer, respectively. Substituting eqs. (3) and (5) into eq. (4), the following relation is obtained:

$$\frac{h_a}{b}\left(\frac{\partial q}{\partial t} + \frac{q}{\tau_a}\right) = E_{a12} \frac{\partial v_a}{\partial t} + \frac{E_{a2}}{\tau_a} v_a, \tag{6}$$

where, $E_{a12} = E_{a1} + E_{a2}$, that is, instantaneous elasticity of adhesive layer. Since the deflection $v_2$ of neutral axis in region-2 is sum of the elongation in y-direction of wood $v_w$ and that of adhesive layer $v_a$, the relation among $v_a$, $v_2$, and q is expressed by using eqs. (1), (2), and (3) as follows:

$$v_a = v_2 - \frac{0.5h_w}{E_y b} q. \tag{7}$$

Substituting eq. (7) into eq. (6), we get

$$\frac{\partial v_2}{\partial t} + \frac{\theta}{\tau_a} v_2 = \frac{h_w}{E_y b}(0.5 + kr) \frac{\partial q}{\partial t} + \frac{h_w}{E_y b \tau_a}(0.5\theta + kr) q, \tag{8}$$

where,

$$\theta = E_{a2}/E_{a12}, \quad k = h_a/h_w, \quad \text{and} \quad r = E_y/E_{a12}.$$

On the other hand, region-2 is also considered as elastic beam subjected to distributed force $-q = -q(x, t)$, so that the following differential equation for the deflection of neutral axis is obtained:

$$E_x I \frac{\partial^4 v_2}{\partial x^4}(x, t) + q(x, t) = 0, \tag{9}$$

where, $E_x$ and I are modulus of elasticity of wood adherend in x-direction and

moment of inertia of beam ($=bh_w^3/12$), respectively. Eliminating the distributed force $q(x, t)$ from eqs. (8) and (9), the following partial differential equation for $v_2$ is obtained.

$$\frac{\partial^5 v_2}{\partial x^4 \partial t}+\alpha\beta\frac{\partial^4 v_2}{\partial x^4}+4\lambda^4\frac{\partial v_2}{\partial t}+4\lambda^4\alpha\theta v_2=0, \tag{10}$$

where,

$$(1/\lambda h_w)^4=(E_x/E_y)(kr+0.5)/3,$$

$$\beta=(\lambda/\gamma)^4,$$

$$(1/\gamma h_w)^4=(E_x/E_y)(kr+0.5\theta)/3,$$

and

$$\alpha=1/\tau_a. \tag{11}$$

*Continuity between Region-1 and Region-2 and Out Line of Numerical Method*

In Fig. 2, region-1 is considered as a cantilever beam subjected to unknown shear force $P(t)$ at $x=-a$. Denoting the slope and deflection at $x=0$ as $\theta_0(t)$ and $v_0(t)$, deflection $v_1$ of the neutral axis in region-1 is expressed as:

$$v_1(x, t)=\frac{P(t)}{E_x I}\left(\frac{x^3}{6}+\frac{ax^2}{2}\right)+\theta_0(t)x+v_0(t). \tag{12}$$

Considering the additional deflection by shear stress, the deflection at loading point of $x=-a$ is expressed as:

$$\frac{\delta}{2}=\frac{St}{2}=\frac{P(t)}{3E_x I}(a^3+\phi a)-\theta_0(t)a+v_0(t), \tag{13}$$

where, $\delta$ is opening distance of DCB specimen at loading point, which is called just "deflection" after this. S is constant cross head speed of the testing machine, $\phi=0.3(E_x/G_{xy})h_w^2$, and $G_{xy}$ is shear rigidity of wood.

The boundary conditions for solving eq. (10) are presented as follows:

at $x=0$,

$$E_x I\frac{\partial^3 v_2}{\partial x^3}=P(t), \quad E_x I\frac{\partial^2 v_2}{\partial x^2}=P(t)a, \tag{14}$$

and, at $x=l$,

$$\frac{\partial^3 v_2}{\partial x^3}=\frac{\partial^2 v_2}{\partial x^2}=0. \tag{15}$$

The boundary conditions involve the unknown function $P(t)$ which is the final object to be determined in this study, so that it is difficult or may be impossible to solve the eq. (10) directly in the closed form. Hence, the eq. (10) was replaced by the finite difference equations and appropriate load increment $\Delta P$ was assumed within a short time interval $\Delta t$ to solve the finite difference equations as a linear simultaneous equations. Then the obtained slope $\theta_0(t)$ and deflection $v_0(t)$ at $x=0$, and assumed load increment $\Delta P$ were substituted into eq. (13) to check the continuity between region-1 and region-2. If the difference between both sides of eq. (13) was larger than an allowable error, iteration of calculation was done on different $\Delta P$ till the best load increment, which satisfied the coincidence of both sides of equation (13), was obtained. This iteration was done from $t=0$ till fracture time. Details of the numerical method are shown in APPENDIX-A.

*Estimation of Fracture Toughness from nonlinear P-δ Relation*

The computed reaction force P(t) was expressed as the following output form

$$\left(1-\frac{P(t)}{P_e}\right)=AB\delta^{BB}, \tag{16}$$

where, $P_e$ is elastic reaction force obtained on the DCB specimen with elastic adhesive layer[1], that is, whose viscous term $\tau_a$ is neglected, and expressed as:

$$P_e=1.5E_xI\cdot\delta/f_e(a), \tag{17}$$

$$f_e(a)=a^3+\phi a+3a^2/\lambda+3a/\lambda^2+1.5/\lambda^3. \tag{18}$$

In the eq. (16), variables AB and BB were determined by the least squares method, and it appeared from a series of computations that these variables were also functions of beam length "a".

Therefore, variables AB and BB were also fitted against the beam length "a" with n-th order polynominals of "a" by the least squares method. As the results of these fitting operations, P−δ relation was expressed as the following form:

$$P(\delta)=1.5E_xI\delta(1/f_e(a)-F_1(a)\delta^{F_2(a)}), \tag{19}$$

where, functions $F_1(a)$ and $F_2(a)$ took the following general forms;

$$F_1(a)=\sum_{i=0}^{n}C_ia^i, \tag{20}$$

$$F_2(a)=\sum_{i=0}^{n}K_ia^i. \tag{21}$$

The strain energy stored in the specimen from beginning of loading till the fracture is calculated by using eq. (19) as follows:

$$U_c(a)=\int_0^{\delta c}P(a,\delta)\,d\delta=1.5E_xI\delta_c^2\left\{\frac{1}{2f_e(a)}-\frac{F_1(a)}{F_2(a)+2}\delta_c^{F_2(a)}\right\}, \tag{22}$$

where, $\delta_c$ is deflection at the fracture.

The definition of the fracture toughness is

$$G_c=-\frac{1}{b}\cdot\frac{dU_c(a)}{da}. \tag{23}$$

Thus, the following equation for estimating fracture toughness $G_c$ is obtained from eqs. (22) and (23),

$$G_c=1.5E_xI(\delta_c^2/b)(\Gamma_e(a)+\Gamma_v(a)), \tag{24}$$

where, function $\Gamma_e(a)$ is the term of elastic contribution and expressed as:

$$\Gamma_e(a)=f_e'(a)/2f_e(a)^2, \tag{25}$$

and, function $\Gamma_v(a)$ is the term of viscoelastic contribution and expressed as:

$$\Gamma_v(a)=\frac{\delta_c^{F_2(a)}}{[F_2(a)+2]^2}\{[F_2(a)+2][F_1'(a)+F_1(a)F_2'(a)\log_e\delta_c]-F_2'(a)F_1(a)\}, \tag{26}$$

where, dash denotes the first derivative with respect to "a". It was suggested that estimation of $G_c$ of individual DCB specimen should be done with individual flexural rigidity peculiar to each specimen obtained from linear portion of each

P−$\delta$ curve. Therefore, $G_c$ is also estimated with following equation:

$$G_c=\left(\frac{f_e(a)}{COMP_{exp}}\right)\left(\frac{\delta_c^2}{b}\right)(\Gamma_e(a)+\Gamma_v(a)), \tag{27}$$

where, $COMP_{exp}$ indicates compliance defined as $\delta/P$ of each specimen obtained experimentary, and is related with the theoretical flexural rigity $E_xI$ through eq. (17) as follows:

$$E_xI=f_e(a)/1.5COMP_{exp}. \tag{28}$$

*Another Methods Depending on Linear Assumption*

Both eqs. (24) and (27) were derived on the exact deffinition of strain energy release rate, so that they included only deflection $\delta_c$ at fracture, because the argument of strain energy is deflextion as shown in eq. (22). If, howevere, P−$\delta$ relation could be considered as linear, strain energy is equivalent to complementary energy defined as follows:

$$V_c(P_c, a)=\int_0^{P_c}\delta(P, a)dP \tag{29}$$

Thus, in case of linear P−$\delta$ relation, critical strain energy release rate $G_c$ is equivalent to critical complementary energy release rate, which is defined as follows:

$$G_c=\frac{1}{b}\cdot\frac{dV_c(a)}{da}=\frac{1}{b}\cdot\frac{d}{da}\int_0^{P_c}\delta(P, a)dP. \tag{30}$$

Substituting eq. (17) into eq. (30), we get an another equation for estimating $G_c$ as follows:

$$G_c=\frac{P_c^2}{3bE_xI}f_e'(a). \tag{31}$$

Equation (31) is well known one usually derived from the complince, and was used in the authors' previous paper[1] too. This eq. (31) is also modified with the relation of eq. (28) as follows:

$$G_c=\frac{P_c^2}{2b}\cdot\frac{f_e'(a)}{f_e(a)}COMP_{exp}. \tag{32}$$

On the other hand, Sasaki[2] had presented a similar but slight different equation to eq. (32) as follows:

$$G_c=\frac{P_c\delta_c}{2b}\cdot\frac{f_e'(a)}{f_e(a)}. \tag{33}$$

In the eq. (33), the compliance $COMP_{exp}$ in eq. (32) was replaced by the ratio of deflection $\delta_c$ at fracture and fracture load $P_c$. In this study, $G_c$ was estimated with every equation presented here, and the difference among the estimation methods was discussed.

## Experimental

*Materials*

Wood: Air dried Japanese red pine (*Pinus densiflora* Sieb. et Zucc.) was used as

the adherend. Mechanical properties of the wood $E_L(E_x)$, $E_T(E_y)$, and $E_{LT-45°}$ ($E_{xy-45°}$) were measured on small clear specimens by the compression test. Poisson's ratio $\mu_{LT}(\mu_{xy})$ was quated from the data book[3] and shear rigidity $G_{LT}(G_{xy})$ was calculated by using Jenkin's equation. These results are tabulated in Table 1.

Adhesives: Epoxy adhesives were used. Base resin was a mixture of bisphenol-A of WPE* 180~190 and dibutylphthalate. Every 0, 20, 40, and 60 phr** of polysulfide was added to the base resin as flexibilizer. Each mixture was cured with 11 phr of diethylenetriamine (DETA) at room temperature. These epoxy adhesives containing n-phr of flexibilizer were denoted as EP-n. In this study, four kinds of epoxy adhesives, EP-0, EP-20, EP-40, and EP-60 were presented.

*Preparation of DCB Specimen*

DCB specimens as shown in Fig. 1 were prepared in accordance with the method presented in the previous paper[1]. The span of the cantilever beam "a" was varied from 3 cm to 13 cm at an interval of 2 cm. Thickness of adhesive layer $2h_a$ was adjusted by polyethylene spacer shims of 0.15 cm thick. Depth $h_w$ and thickness b of the cantilever beam were 1.5 cm and 1.0 cm respectively. Total length of specimen $(a+l)$ was constant of 20 cm through all specimens.

*Creep Test on Cast Epoxy Specimen*

In this study, the mechanical behaviour of epoxy adhesive was simulated by the three element model constituted by parallel row of a Maxwell model and a elastic spring as shown in Fig. 2. In order to determine the constants $E_{a1}$, $E_{a2}$, and $\tau_a$ of the model, tensile creep tests were carried out on cast epoxy specimens.

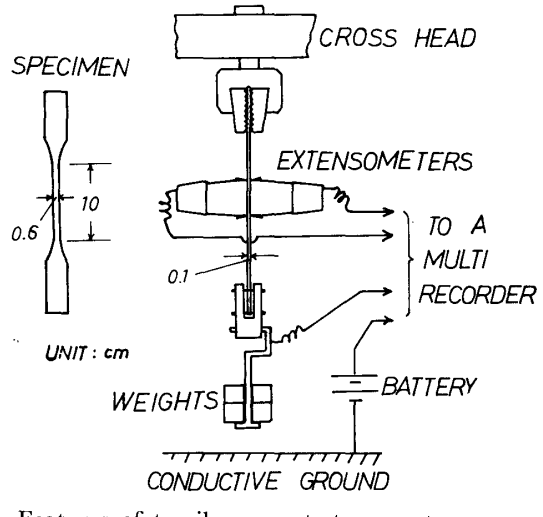


Fig. 3. Features of tensile creep test on cast epoxy specimen.

* WPE: weight per epoxy equivalent.

** phr: parts per hundred of resin by weight.

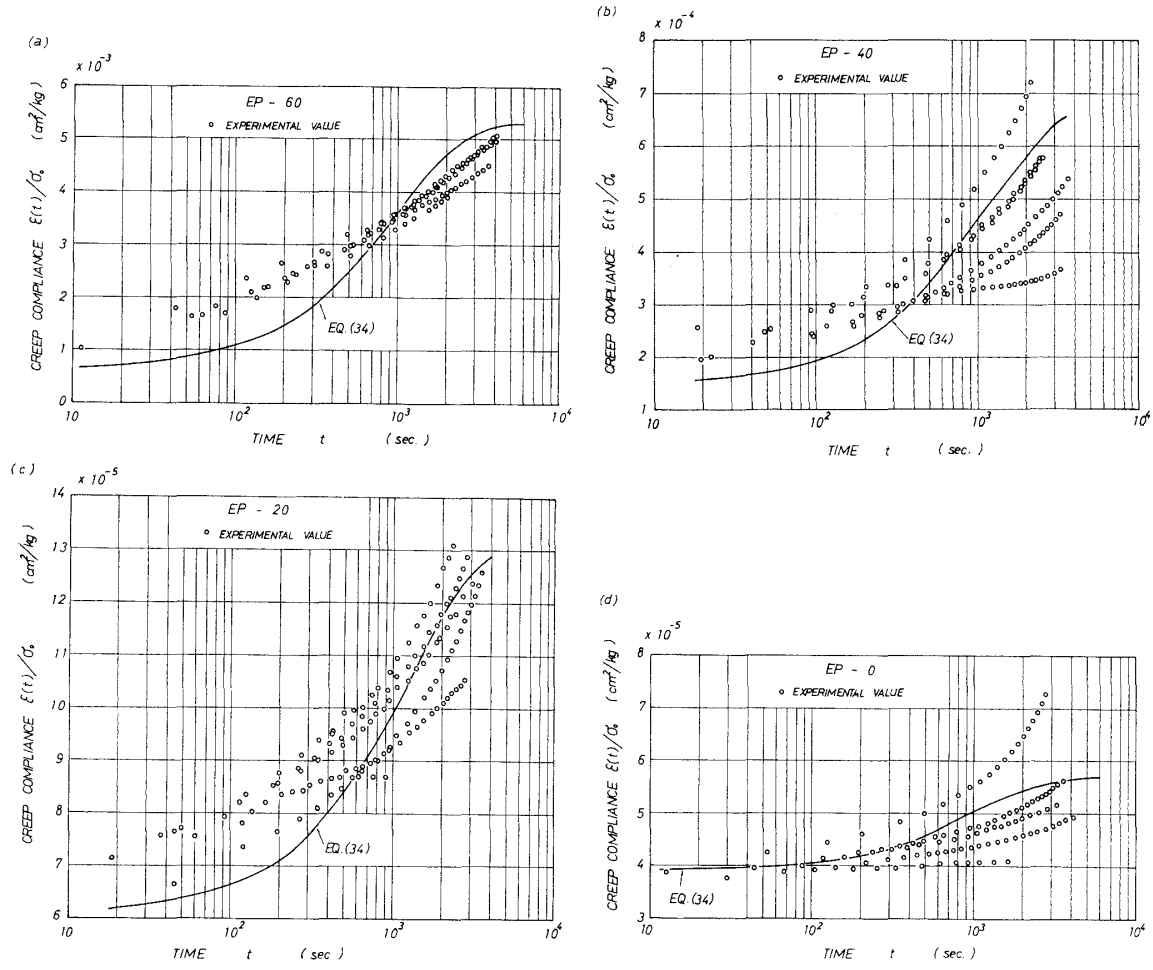


Fig. 4. Results of tensile creep tests on cast epoxy specimens.

Fig. 3 shows the schematic feature of the creep test. A circuit was set to catch the beginning of loading as shown in Fig. 3. The constants of the model were determined so as to satisfy the following equation of creep compliance derived from the differential equation (4).

$$\varepsilon_a(t)/\sigma_0=\frac{1}{E_{a2}}\left\{1-\frac{E_{a1}}{E_{a12}}\exp\left(-\frac{E_{a2}t}{E_{a12}\tau_a}\right)\right\}, \qquad (34)$$

where, $\sigma_0$ is applied stress. The details of the fitting operation of the constants are shown in APPENDIX-B. Table 2 shows the obtained mechanical properties of cast epoxy adhesives. Figs. 4(a)~(d) show the results of creep tests and fitted creep compliance $\varepsilon_a(t)/\sigma_0$ calculated by substituting the obtained mechanical properties to eq. (34). It appeared from these results that the behaviour of real epoxy adhesive can not be simulated exactly by a simple model like the three elements model. In this study, however, three elements model dared to be used for simplicity of the analysis.

*Fracture Toughness Test*

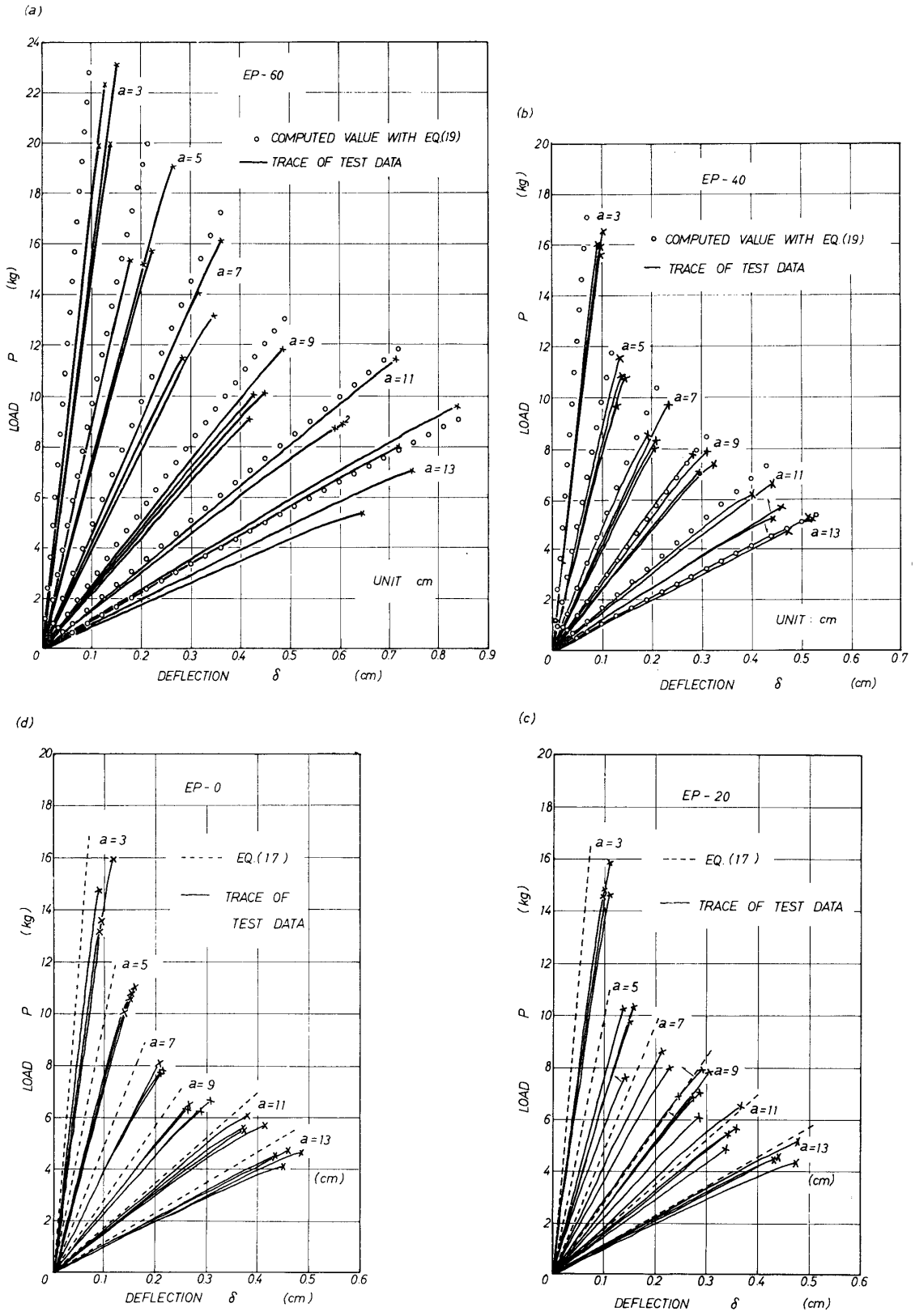


Fig. 5. P--$\delta$ relations of real DCB specimens and of simulated ones. Small number 2 in Fig. 5(a) indicates that there are two same test results.

Fracture toughness tests were done on an Instron type testing machine (TOM 200J, Shinko Communication Ind. Ltd.). Load-deflection curves were recorded on a XY-recorder. Original load-deflection curve on the XY-recorder was S-shaped curve, which was interpreted by both the looseness of attachments at the beginning of loading and essential nonlinear behaviour of the specimen. Therefore, to eliminate the effect of the looseness of attachments, the foot part of this S-shaped original curves was corrected by an extension line of the linear portion of the curves, then these load-deflection data were put into a computer to calculate the fracture toughness. All tests were done in a room conditioned at about 20°C, 65 % R.H., and under the constant cross head speed of 0.1 cm/min.

## Results and Discussion

*Load-Deflection Relation*

As the results of a series of computer simulations, it appeared that while the $P-\delta$ relations in cases of EP-0 and EP-20 could be regarded as linear, that in cases of EP-40 and EP-60 showed a slight nonlinearity. Therefore, considerations for nonlinearity of $P-\delta$ relation were only given on the cases of EP-40 and EP-60, and anothers were treated as the specimens with elastic adhesive layer. Figs. 5-(a), (b), (c), and (d) show the comparisons between $P-\delta$ curves of real specimens and computed ones. Computations were done with linear equation (17) in cases of both EP-0 and EP-20, on the other hand, in cases of both EP-40 and EP-60, computations were done with nonlinear equation (19). All computations were

Table 1. Mechanical properties of wood adherend.

| $E_L$ (kg/cm²) $\times 10^3$ | | $E_T$ (kg/cm²) $\times 10^3$ | | $E_{LT-45°}$ (kg/cm²) $\times 10^2$ | | $\mu_{LT}$[3] | $G_{LT}$* (kg/cm²) $\times 10^3$ |
|---|---|---|---|---|---|---|---|
| m | s.d | m | s.d | m | s.d | | |
| 111.5 | 21.4 | 6.8 | 0.4 | 10.6 | 2.4 | 0.6 | 4.3 |

* $1/G_{LT}=4/E_{LT-45°}-1/E_L-1/E_T+2\mu_{LT}/E_L$, m; mean, s.d; standard deviation.

Table 2. Mechanical properties of cast epoxy adhesives.

| EP−n | $E_{a1}$ (kg/cm²) | | $E_{a2}$ (kg/cm²) | | $\tau_a$ (sec.) | |
|---|---|---|---|---|---|---|
| | m | s.d | m | s.d | m | s.d |
| 60 | 1393.0 | 234.5 | 188.0 | 20.8 | 117.1 | 18.8 |
| 40 | 5310.7 | 869.8 | 1501.5 | 547.2 | 231.3 | 67.6 |
| 20 | 8798.0 | 3092.6 | 7578.3 | 2150.8 | 583.0 | 62.6 |
| 0 | 8009.6 | 4634.0 | 17522.0 | 4688.6 | 703.9 | 351.1 |

m; mean, s.d; standard deviation.

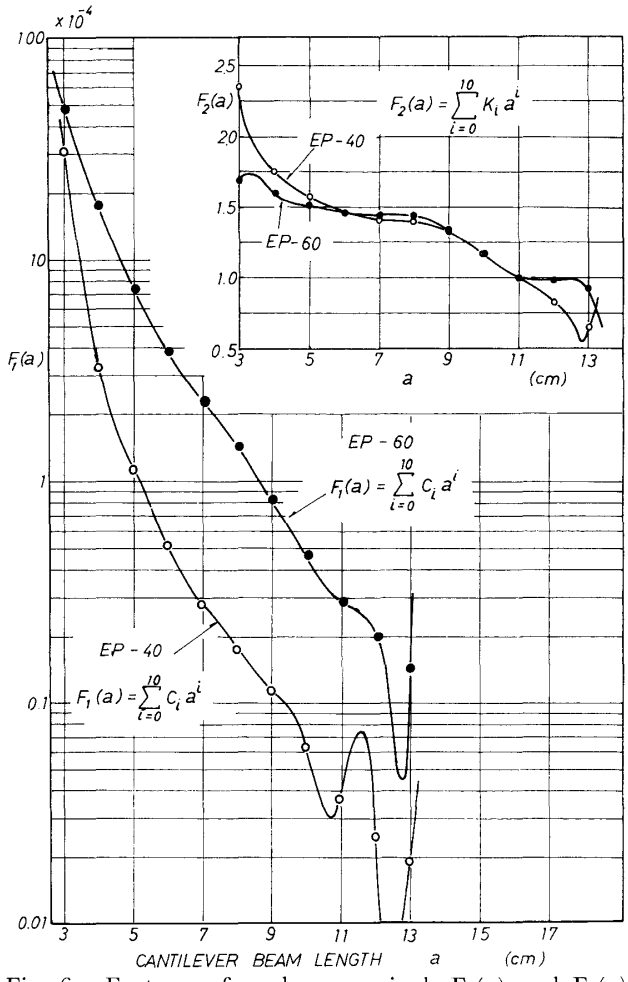


Fig. 6. Features of used poynominals $F_1(a)$ and $F_2(a)$.

done by substituting the avarage size of specimens in every group of the same beam length and mechanical properties tabulated in Tables 1 and 2. Features of used polynominals $F_1(a)$ and $F_2(a)$ are shown in Fig. 6.

As can be seen in Figs. 5-(a)～(d), behaviour of real specimens is more flexible than that of simulated models as the beam length becomes short. These disagreements are supposed to arise partly from an over estimation of Young's modulus $E_x$ wood, and partly from the fact that actual DCB specimens did not behave as cantilever beams expecting from the elementaly beam theory, especially when beam length becomes very short. Therefore, it is necessary for the estimation of fracture toughness to correct these disagreements. This correction could easily be done by using the apparent flexural rigidity shown in eq. (28) instead of using a theoretical one $E_xI$. Figs. 7-(a), (b), (c), and (d) show the comparison of measured strain energy with calculated one. The calculations of strain energy were done on the eq. (22) by using alternately a theoretical flexural rigidity $E_xI$ and the apparent one corrected with $COMP_{exp}$ as shown in eq. (28). It can be seen in these figures

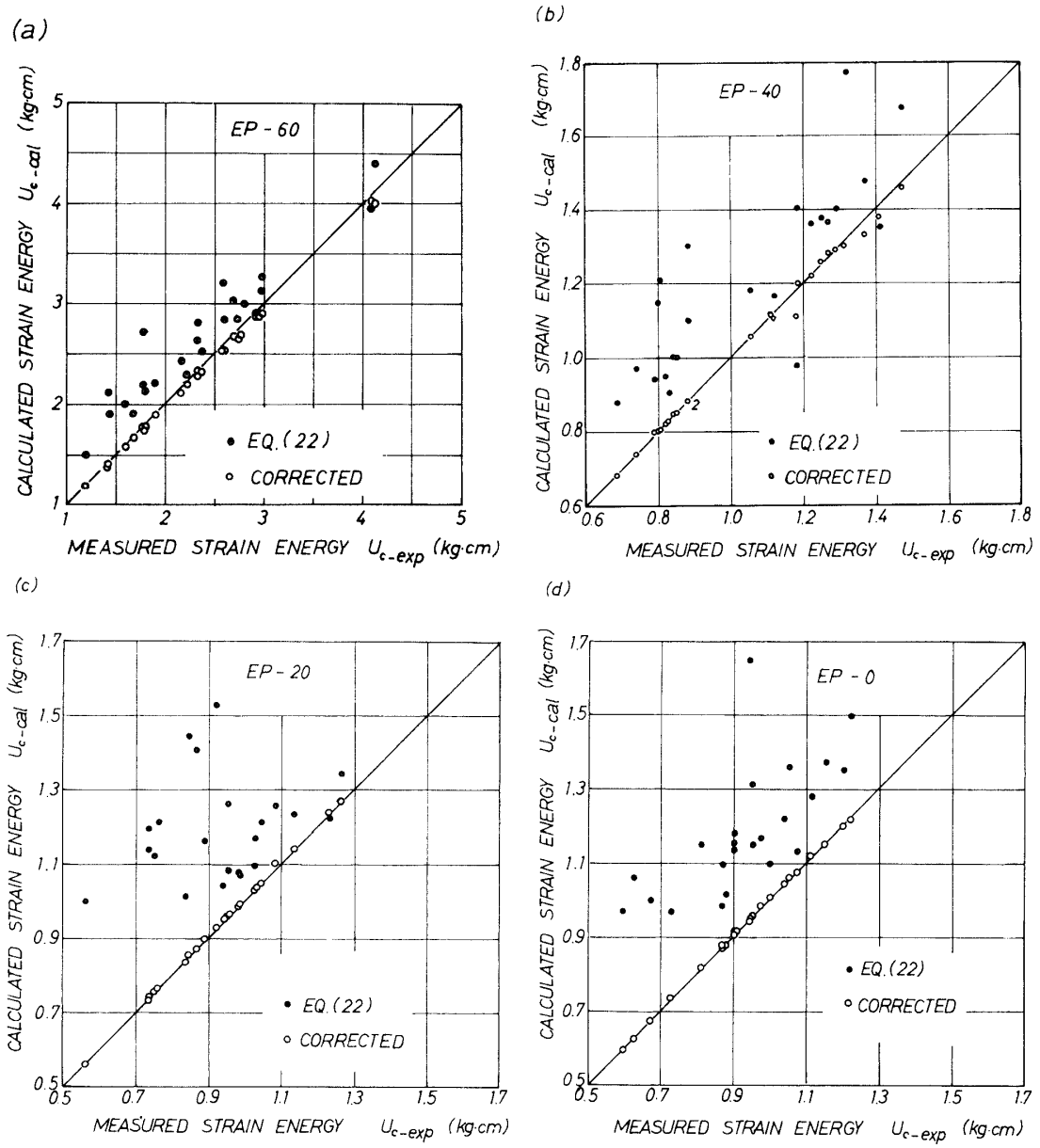


Fig. 7. Comparison of measured strain energy stored in the specimen from the begining of loading till the fracture with calculated one.

that the correction by using the apparent flexural rigidity gives good results for the estimation of strain energy of each specimen, so that same efficiency is expected on estimation of the fracture toughness.

*Observation of Fracture Phenomena with Eyes.*

In cases of EP-0 and EP-20, almost all cracks extended slowly and sluggishly toward the end of glue line as the opening of specimen increased. Micro-cracks grew always prior to a relatively large crack proprgation, so that P—$\delta$ curve did not have clear peaks which indicate the beginnings of rapid crack propagation.

Crack propagation was limitted within the vicinities of the interface of adhesive and adherend, and specimen did not be separated into two parts.

On the other hand, in case of EP-60, specimens were very tough compared with other groups. Fracture occured suddenly and with one rush specimen separated perfectly into two parts. Growth of micro-cracks prior to the breakdown of specimen was hardly observed with eyes. Therefore, almost all $P-\delta$ curves had a clear peak at the fracture initiation.

In case of EP-40, fracture phenomena were, if anything, close to those of EP-0 and EP-20.

*Fracture Toughness*

Fracture toughness $G_c$ was estimated with various equations shown as follows:

$$G_{c-1}=1.5E_xI(\delta_c^2/b)[\Gamma_e(a)+\Gamma_v(a)] \quad \text{viscoelastic,}$$

$$G_{c-2}=1.5E_xI(\delta_c^2/b)\Gamma_e(a) \quad \text{elastic,}$$

$$G_{c-3}=\frac{f_e(a)}{COMP_{exp}}(\delta_c^2/b)[\Gamma_e(a)+\Gamma_v(a)] \quad \text{viscoelastic,}$$

$$G_{c-4}=\frac{f_e(a)}{COMP_{exp}}(\delta_c^2/b)\Gamma_e(a) \quad \text{elastic,}$$

$$G_{c-5}=\frac{P_c^2}{3bE_xI}f_e'(a) \quad \text{elastic,}$$

$$G_{c-6}=\frac{P_c^2}{2b}\frac{f_e'(a)}{f_e(a)}COMP_{exp} \quad \text{elastic,}$$

$$G_{c-7}=\frac{P_c\delta_c}{2b}\frac{f_e'(a)}{f_e(a)} \quad \text{elastic,}$$

Calculated results are shown in Table 3. Each value in this table indicates the mean of four specimens belonging to a group of the same size. Calculations of the total mean value within each adhesive group were done, in which the values for the cases of a=3 cm and a=13 cm were excluded, because it was supposed that the former had influence of the loading points, and the latter had influence of the free end. In Table 3, the values of fracture toufihness $G_{c-1}$ and $G_{c-3}$ estimated on the groups of a=13 cm showed a little strange values compared with the other cases. These phenomena might be interpreted as the oscilative characters of used polynominals $F_1(a)$ and $F_2(a)$ as shown in Fig. 6.

Fig. 8 shows plots of mean fracture toughness to the flexibilizer content. It is clear from this figure that the fracture toughntss $G_{c-1}$, $G_{c-2}$, and $G_{c-5}$ which involve theoretical flexural rigidity $E_xI$ take the two extremes among seven kinds of fracture toughness. These results can be understood as the matter of course coming from an over estimation of Young's modulus $E_x$ of wood adherends as already mentioned. On the other hand, the fracture toughness $G_{c-3}$, $G_{c-4}$, $G_{c-6}$, and $G_{c-7}$, whose flexural rigidity were corrected with experimental data, took the intermediate

Table 3. Fracture toughness estimated with various methods (kg.cm/cm$^2$).

| EP—n | a (cm) | $G_{c-1}$ | $G_{c-2}$ | $G_{c-3}$ | $G_{c-4}$ | $G_{c-5}$ | $G_{c-6}$ | $G_{c-7}$ |
|---|---|---|---|---|---|---|---|---|
| 60 | 3 | 0.946 | 1.030 | 0.666 | 0.724 | 0.487 | 0.689 | 0.722 |
| | 5 | 0.894 | 0.929 | 0.734 | 0.762 | 0.590 | 0.716 | 0.745 |
| | 7 | 0.736 | 0.763 | 0.657 | 0.681 | 0.584 | 0.651 | 0.669 |
| | 9 | 0.628 | 0.654 | 0.545 | 0.567 | 0.476 | 0.548 | 0.559 |
| | 11 | 0.703 | 0.709 | 0.639 | 0.644 | 0.567 | 0.623 | 0.634 |
| | 13 | 1.113 | 0.572 | 1.051 | 0.542 | 0.491 | 0.513 | 0.528 |
| Total mean* | | 0.740 | 0.763 | 0.644 | 0.664 | 0.554 | 0.635 | 0.652 |
| C.V. (%) | | 23.0 | 23.4 | 22.6 | 22.8 | 23.7 | 21.8 | 22.4 |
| 40 | 3 | 0.581 | 0.579 | 0.406 | 0.405 | 0.268 | 0.382 | 0.401 |
| | 5 | 0.360 | 0.360 | 0.295 | 0.295 | 0.220 | 0.268 | 0.283 |
| | 7 | 0.327 | 0.327 | 0.276 | 0.277 | 0.224 | 0.264 | 0.271 |
| | 9 | 0.316 | 0.316 | 0.296 | 0.296 | 0.259 | 0.276 | 0.286 |
| | 11 | 0.352 | 0.335 | 0.298 | 0.284 | 0.230 | 0.269 | 0.277 |
| | 13 | 0.668 | 0.242 | 0.650 | 0.236 | 0.220 | 0.223 | 0.229 |
| Total mean* | | 0.339 | 0.335 | 0.291 | 0.288 | 0.233 | 0.269 | 0.280 |
| C.V. (%) | | 13.4 | 13.1 | 10.9 | 10.9 | 12.9 | 10.0 | 10.4 |
| 20 | 3 | | 0.674 | | 0.416 | 0.237 | 0.384 | 0.407 |
| | 5 | | 0.405 | | 0.272 | 0.174 | 0.257 | 0.266 |
| | 7 | | 0.439 | | 0.303 | 0.198 | 0.279 | 0.292 |
| | 9 | | 0.289 | | 0.252 | 0.207 | 0.236 | 0.244 |
| | 11 | | 0.229 | | 0.211 | 0.189 | 0.204 | 0.208 |
| | 13 | | 0.220 | | 0.202 | 0.174 | 0.189 | 0.196 |
| Total mean* | | | 0.341 | | 0.259 | 0.192 | 0.244 | 0.251 |
| C.V. (%) | | | 31.4 | | 18.6 | 19.2 | 17.1 | 18.2 |
| 0 | 3 | | 0.591 | | 0.358 | 0.207 | 0.341 | 0.354 |
| | 5 | | 0.429 | | 0.319 | 0.210 | 0.283 | 0.302 |
| | 7 | | 0.335 | | 0.267 | 0.185 | 0.233 | 0.250 |
| | 9 | | 0.280 | | 0.232 | 0.178 | 0.213 | 0.223 |
| | 11 | | 0.274 | | 0.239 | 0.195 | 0.222 | 0.231 |
| | 13 | | 0.227 | | 0.197 | 0.160 | 0.185 | 0.191 |
| Total mean* | | | 0.329 | | 0.286 | 0.192 | 0.250 | 0.252 |
| C.V. (%) | | | 22.8 | | 33.2 | 8.9 | 23.2 | 15.3 |

C.V. coefficient of variation = (standard deviation ÷ mean value) × 100

* Total mean was calculated by omitting the values for the cases of a = 3 cm and a = 13 cm.

values. Considering these results, it is reasonable to suppose that the latter four kinds of fracture toughness are the reliable values of fracture toughness of wood (Japanese red pine)-epoxy adhesives systems. Among these four kinds of fracture toughness supposed to be reliable, $G_{c-3}$ is the only one estimated through viscoelastic

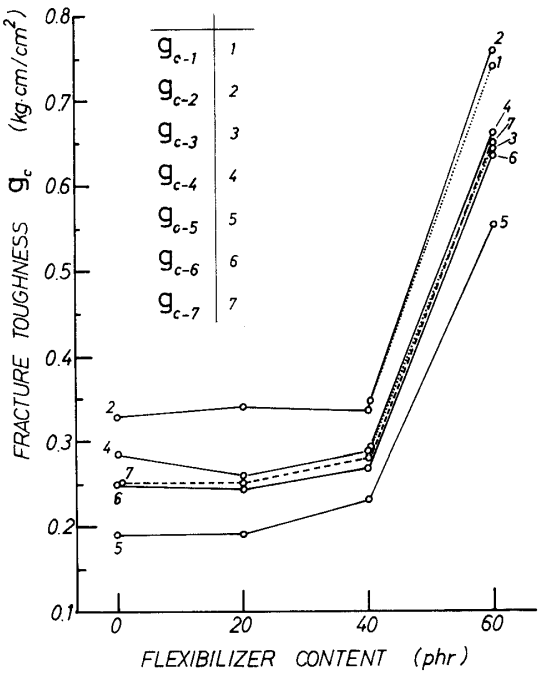


Fig. 8. Relation between fracture toughness and flexibilizer content for various estimation methods. Each plot is total mean of fracture toughness within each adhesive group.

assumption. If this value is assumed to be the most close to real fracture toughness being affected by viscoelastic behaviour of adhesive layer, it will be concluded in the extent of this experiment that there are no essential distinctions between two kinds of fracture toufihness estimated through viscoelastic and elastic assumptions. This means that the methods based on the elastic assumption are reliable enough for estimating the fracture toughness of DCB specimens whose load-deflection relations show slight nonlinearity. Moreover, among these estimation methods based on the elastic assumption, the method for $G_{c-7}$ is recommended as the most simplest and convenient method which can implicitly involve the nonlinear contribution on the fracture toughness of DCB specimen.

## Conclusion

(1) There were no essential distinctions between two kinds of fracture toughness estimated with time dependent equation in which the adhesive layer of Double Cantilever Beam (DCB) specimen was simulated fly infinite rows of three elements model and with time independent equation in which the adhesive layer of the specimen was simulated by infinite rows of elastic springs.

(2) It is undesirable for the estimation of fracture toughness of DCB specimen to use the equation including an average flexural rigidity $E_xI$ of cantilever beam

calculated theoretically, because each specimen has always some amount of scatter in the mechanical properties and the sizes. On the other hand, the estimation method involving individual flexural rigidity corrected fly compliance measured on each specimen gives reliable values of fracture toughness, though a little trouble may exist in the process of determing the compliance.

(3) In case of DCB specimen of which load-deflection relation shows a little nonlinearity, the estimation method derived by Sasaki which involves data of load and deflection at the fracture gives reliable values of fracture toufihness with less trouble and scatter, and is recommended as the most convenient way.

## APPENDIX-A

*Numerical Method for Obtaining Reaction Force P(t)*

The partial differential equation to be solved is

$$\frac{\partial^5 v_2}{\partial x^4 \partial t}+\alpha\beta\frac{\partial^4 v_2}{\partial x^4}+4\lambda^4\frac{\partial v_2}{\partial t}+4\lambda^4\alpha\theta v_2=0. \tag{A1}$$

The boundary conditions are

$$E_x I\frac{\partial^3 v_2}{\partial x^3}(0,\,t)=P(t),\quad E_x I\frac{\partial^2 v_2}{\partial x^2}(0,\,t)=P(t)a, \tag{A2}$$

$$\frac{\partial^3 v_2}{\partial x^3}=0,\quad \frac{\partial^2 v_2}{\partial x^2}=0.\quad (x=l) \tag{A3}$$

The continuity between region-1 and region-2 is checked with following equation:

$$\frac{\delta}{2}=\frac{St}{2}=\frac{P(t)}{3E_x I}(a^3+\phi a)-\theta_0(t)a+v_0(t), \tag{A4}$$

where, $\theta_0(t)=\frac{\partial v_2}{\partial x}(0,\,t)$, $v_0(t)=v_2(0,\,t)$, and $\delta$ is the deflection prescrived by the movement of cross head of which speed is S.

As shown in Fig. A1 the region-2 was divided at regular intervals in $m$ mesh points. Where, $\zeta$ is interval of the mesh points and I, II, III, and IV are the imaginary points added for expressing the boundary conditions. Using the central difference with x and the forward difference with t, eq. (A1) is transformed into following finite difference equation on every point $k(1\leqq k\leqq m)$ in Fig. A1.

$$V_{k+2}-4V_{k+1}+(6+4\lambda^4\zeta^4)V_k-4V_{k-1}+V_{k-2}=(1-\Delta t\alpha\beta)\bar{V}_{k+2}-4(1-\Delta t\alpha\beta)\bar{V}_{k+1}$$

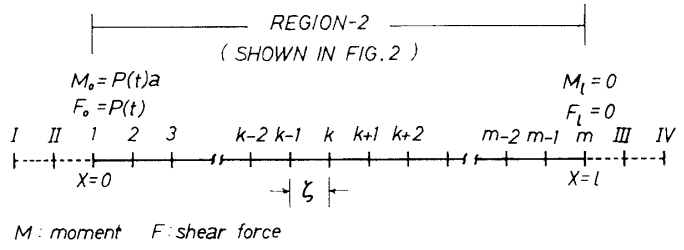


Fig. A1. Mesh separation of region-2 and boundary conditions.

$$+\{(6+4\lambda^4\zeta^4)-\Delta t\alpha\beta(6+4\gamma^4\zeta^4\theta)\}\bar{V}_k-4(1-\Delta t\alpha\beta)\bar{V}_{k-1}+(1-\Delta t\alpha\beta)\bar{V}_{k-2}, \quad (A5)$$

where, $\gamma^4=\lambda^4/\beta$, and $V_k$, $\bar{V}_k$ and $\Delta t$ are defined as follows:

$$\frac{\partial v_2}{\partial t}=\frac{\partial V}{\partial t}\Big|_k \fallingdotseq \frac{V_k(t+\Delta t)-V_k(t)}{\Delta t}=\frac{V_k-\bar{V}_k}{\Delta t}. \quad (A6)$$

Considering the boundary conditions of eq. (A2) and (A3), the deflections on the imaginary points are expressed with deflections on inner points and unknown force P(t) as follows:

$$V_I = 2V_1-V_2+\frac{P(t)a\zeta^2}{E_xI}, \quad (A7)$$

$$V_{II} = 4V_1-4V_2+V_3+\frac{2P(t)(a-\zeta)\zeta^2}{E_xI}, \quad (A8)$$

$$V_{III}=2V_m-V_{m-1}, \quad (A9)$$

$$V_{IV}=V_{m-2}-V_{m-1}+4V_m. \quad (A10)$$

Then, the following $m\times m$ simultaneous equations are obtained by constructing eq. (A5) on every inner mesh point of $k=1\sim m$ with eqs. (A7)$\sim$(A10).

$$[R_{ij}]\{V_j\}=[\bar{R}_{ij}]\{\bar{V}_j\}+\{Q_i\}, \quad (A11)$$

$$i, j=1\sim m,$$

where, matrics $[R_{ij}]$ and $[\bar{R}_{ij}]$ are band matrics having the following non-zero components:

$$R_{1,1}=R_{m,m}=A-4,$$
$$R_{1,2}=R_{2,3}=R_{k,k-1}=R_{k,k+1}=R_{m-1,m-2}=R_{m,m-1}=-4,$$
$$R_{1,3}=R_{m,m-2}=2,$$
$$R_{2,1}=R_{m-1,m}=-2,$$
$$R_{2,2}=R_{m-1,m-1}=A-1,$$
$$R_{2,4}=R_{k,k-2}=R_{k,k+2}=R_{m-1,m-3}=1,$$
$$R_{k,k}=A,$$

where, $k=3\sim m-2$. (A12)

And,
$$\bar{R}_{1,1}=\bar{R}_{m,m}=A+B-4C,$$
$$\bar{R}_{1,2}=\bar{R}_{2,3}=\bar{R}_{k,k-1}=\bar{R}_{k,k+1}=\bar{R}_{m-1,m-2}=\bar{R}_{m,m-1}=-4C,$$
$$\bar{R}_{1,3}=\bar{R}_{m,m-2}=2C,$$
$$\bar{R}_{2,1}=\bar{R}_{m-1,m}=-2C,$$
$$\bar{R}_{2,2}=\bar{R}_{m-1,m-1}=A+B-C,$$
$$\bar{R}_{2,4}=\bar{R}_{k,k-2}=\bar{R}_{k,k+2}=\bar{R}_{m-1,m-3}=C,$$
$$\bar{R}_{k,k}=A+B,$$

where, $k=3\sim m-2$, and

$$A=6+4\lambda^4\zeta^4, \quad B=-\Delta t\alpha\beta(6+4\gamma^4\zeta^4\theta), \quad \text{and} \quad C=1-\Delta t\alpha\beta. \quad (A14)$$

Vectors $\{V_j\}$ and $\{\bar{V}_j\}$ are correspond to $\{V_1, V_2, \cdots V_k, \cdots V_m\}^T$ and $\{\bar{V}_1, \bar{V}_2, \cdots \bar{V}_k, \cdots \bar{V}_m\}^T$, respectively. Vectors $\{Q_i\}$ involve unknown reaction force P(t) and their non-zero components are

$$Q_1=\frac{2(a+\zeta)\zeta^2}{E_xI}\{\Delta P+\bar{P}(1-C)\}, \tag{A15}$$

$$Q_2=-\frac{a\zeta^2}{E_xI}\{\Delta P+\bar{P}(1-C)\}. \tag{A16}$$

Where, $\Delta P$ and $\bar{P}$ are defined as follows:

$$P(t+\Delta t)-P(t)=P-\bar{P}=\Delta P,$$

that is, $\Delta P$ is load increment within a short time interval $\Delta t$. Simultaneous equations (A11) can be solved when both bectors $\{\bar{V}_j\}$ and $\{Q_i\}$ are known. At the first stage of calculation, $\{\bar{V}_j\}$ and $\bar{P}$ were put equal to zero, and iterative operation for searching the best load increment was continued by using so-called "two device searching method" till the assumed load increment $\Delta P$ satisfied sufficiently the continuity equation (A4). After the first stage, resolved solutions $\{V_j\}$ and determined the best load increment $\Delta P_{best}$ were used for $\{V_j\}$ and $\bar{P}$ in the next stage of iterative calculation. Mesh interval $\zeta$ was controlled so as to be 0.1 cm, so that the maximum number of mesh point m was varied in response to the glue line length $l$. Time interval $\Delta t$ was empirically determined so as to make the maximum loading time equal to the product of $\Delta t$ and 60. The simultaneous equations were resolved with the inverse matrics method under the declaration of double precision. All computations were done on a FACOM 230-75 computer at the computer center of Kyoto University.

## APPENDIX-B

*Determination of Constant of Three Elements Model.*

Time dependent strain $\varepsilon_a(t)$ of the three elements model is expressed by solving the differential equation (4) as follows:

$$\varepsilon_a(t)=\frac{\sigma_0}{E_{a2}}\left\{1-\frac{E_{a1}}{E_{a12}}\exp\left(-\frac{E_{a2}}{E_{a12}\tau_a}t\right)\right\}. \tag{B1}$$

Instantaneous strain at the beginning of loading ($t=0$) was obtained on the creep curve, and this is expressed theoretically as

$$\varepsilon_a(0)=\sigma_0/E_{a12}. \tag{B2}$$

Thus, the substantial creep strain $\varepsilon$ is

$$\varepsilon=\varepsilon_a(t)-\varepsilon_a(0)=\left(\frac{E_{a1}}{E_{a2}}\right)\left(\frac{\sigma_0}{E_{a12}}\right)\left\{1-\exp\left(\frac{-E_{a2}t}{E_{a12}\tau_a}\right)\right\}. \tag{B3}$$

Let's eq. (B3) be supposed to take the following general form:

$$\varepsilon=A(1-e^{-Bt}). \tag{B4}$$

Assuming that the experimental data of creep test can also be expressed in the form like eq. (B4), the following three equations are expected among the experimental data (see Fig. B1):

$$A-\varepsilon_{k-1}=Ae^{-Bt_{k-1}}, \tag{B5}$$

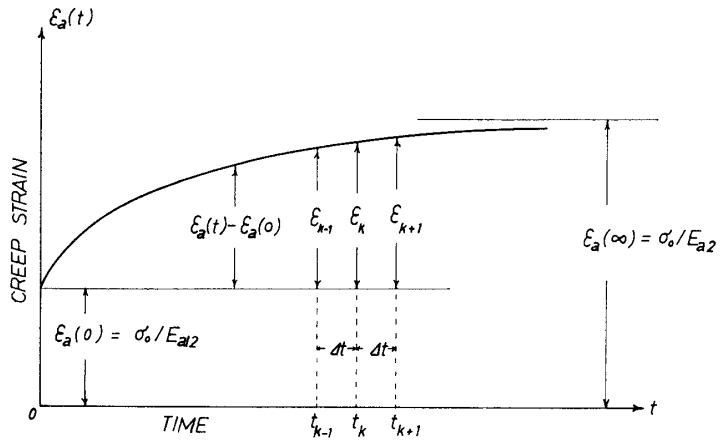


Fig. B1. Schematic explanation for determing constants of three elements model from the creep test data.

$$A-\varepsilon_k=Ae^{-Bt_k}, \tag{B6}$$

$$A-\varepsilon_{k+1}=Ae^{-Bt_{k+1}}, \tag{B7}$$

where, $\varepsilon_{k-1}$, $\varepsilon_k$, and $\varepsilon_{k+1}$ are substantial creep strain obtained from creep test data corresponding to the time of $t_{k-1}$, $t_k$, and $t_{k+1}$ respectively. Where, the time intervals $|t_{k-1}-t_k|$ and $|t_k-t_{k+1}|$ are always taken so as to be equal to a constant interval $\Delta t$. Taking the natural logalism of both sides of eqs. (B5)$\sim$(B7), the following equations are obtained:

$$\log(A-\varepsilon_{k-1})=\log A-Bt_{k-1}, \tag{B8}$$

$$\log(A-\varepsilon_k)=\log A-Bt_k, \tag{B9}$$

$$\log(A-\varepsilon_{k+1})=\log A-Bt_{k+1}. \tag{B10}$$

Then, taking subtraction of eq. (B9) from eq. (B8), as well as, eq. (B10) from eq. (B9), the following equations are obtained:

$$\log\left(\frac{A-\varepsilon_{k-1}}{A-\varepsilon_k}\right)=B(t_k-t_{k-1})=B\Delta t, \tag{B11}$$

$$\log\left(\frac{A-\varepsilon_k}{A-\varepsilon_{k+1}}\right)=B(t_{k+1}-t_k)=B\Delta t. \tag{B12}$$

Thus, the factor A is determined as follows:

$$A=\frac{\varepsilon_k^2-\varepsilon_{k-1}\cdot\varepsilon_{k+1}}{2\varepsilon_k-(\varepsilon_{k-1}+\varepsilon_{k+1})}. \tag{B13}$$

The avarage value of A is obtained by calculating eq. (B13) for every possible combination of $\varepsilon_{k-1}$, $\varepsilon_k$, and $\varepsilon_{k+1}$. At last, the unknown factor B in eq. (B4) is easily obtained after A was known.

## References

1) K. KOMATSU, H. SASAKI and T. MAKU, Wood Research, No. 59/60, 80 (1976).
2) H. SASAKI, Setschaku (Adhesion & Adhesive) (Japan), **18**, 172 (1974).
3) Mokuzai Kogyo Handbook, (Japan), pp. 174 Maruzen, Tokyo, (1973).